

Deep Reinforcement Learning Behavioral Mode Switching Using Optimal Control Based on a Latent Space Objective

Sindre Benjamin Remman, Bjørn Andreas Kristiansen and Anastasios M. Lekkas

Abstract—In this work, we use optimal control to change the behavior of a deep reinforcement learning policy by optimizing directly in the policy’s latent space. We hypothesize that distinct behavioral patterns, termed behavioral modes, can be identified within certain regions of a deep reinforcement learning policy’s latent space, meaning that specific actions or strategies are preferred within these regions. We identify these behavioral modes using latent space dimension-reduction with Pairwise Controlled Manifold Approximation Projection (PaCMAP). Using the actions generated by the optimal control procedure, we move the system from one behavioral mode to another. We subsequently utilize these actions as a filter for interpreting the neural network policy. The results show that this approach can impose desired behavioral modes in the policy, demonstrated by showing how a failed episode can be made successful and vice versa using the lunar lander reinforcement learning environment.

I. INTRODUCTION

Deep reinforcement learning (DRL) has emerged as a powerful paradigm for solving complex decision-making problems, ranging from playing video games [1] to autonomous vehicle control [2]. At the heart of DRL’s success is the ability of neural network policies to learn and adapt to diverse environments through interaction and feedback. However, understanding and interpreting the behavior of these policies remain challenging due to their inherent complexity and the opaque nature of neural networks.

Recent papers such as [3] have shown how neural networks can be used for optimal control, using them as a way to approximate dynamical models and subsequently use them as part of a model-predictive control framework.

This paper analyzes the latent space of neural network policies using the dimension-reduction method PaCMAP [4]. In this case, latent space refers to the activations after the penultimate layer in the neural network policy, visualized in Figure 1. We observe that the policies we consider perform distinct behaviors in separate parts of the latent space. More formally, these neural network policies often perform a specific behavior within certain locations, or hypervolumes, in the policy’s latent space. We call these hypervolumes and their corresponding behavior for *behavioral modes*. We identify behavioral modes in neural network policies trained using DRL and subsequently move the policies between behavioral modes using optimal control with a latent space objective function. More specifically, the contributions of this paper are:

- We use two-dimensional embeddings of DRL policies’ high-dimensional latent space generated using PaCMAP to find situations in different episodes that are initially close in latent space but have different outcomes.

- We employ optimal control to find an action sequence that moves the environment’s state latent space projection closer to a desired part of the latent space, where we hypothesize a desired behavioral mode exists.
- We show results indicating that by moving the environment to a state whose latent space representation is closer to the desired latent space location, we have effectively changed the agent’s behavioral mode.

II. PRELIMINARIES

A. PaCMAP

PaCMAP is a dimension reduction method designed to preserve the original data’s global and local structure in the lower-dimensional embedding. The method was introduced in [4], where the authors compare and analyze several dimension-reduction methods. Based on the insights gained from this analysis, the authors discover helpful design principles for the loss functions used by successful dimension reduction methods. The authors subsequently use these design principles to design the PaCMAP method.

To enable the low-dimensional embedding to preserve the higher-dimensional data local and global structure, PaCMAP uses three different types of point pairs: *neighbor pairs*, which are points that are closest in the original data space, with distance defined using a scaled Euclidean distance function; *mid-near pairs*, which are on average closer in the original data space than random points from the data set; and *further pairs*, which are found by sampling non-neighbors. The loss function used in PaCMAP is

$$\begin{aligned} Loss^{PaCMAP} = & w_{NB} \sum_{i,j \text{ are neighbor pairs}} \frac{\tilde{d}_{ij}}{10 + \tilde{d}_{ij}} \\ & + w_{MN} \sum_{i,j \text{ are mid-near pairs}} \frac{\tilde{d}_{ij}}{10000 + \tilde{d}_{ij}} \\ & + w_{FP} \sum_{i,j \text{ are FP pairs}} \frac{1}{1 + \tilde{d}_{ij}}, \end{aligned}$$

where $\tilde{d}_{ij} = \|\mathbf{y}_i - \mathbf{y}_j\|^2$, and \mathbf{y}_i is the position of data point i in the lower-dimensional embedding. w_{NB} , w_{MN} , and w_{FP} are the weights for the three graph components. These weights are changed throughout the optimization process using a pre-defined strategy. The optimization process aims to preserve the original data’s structure in the lower-dimensional embedding by minimizing the loss function, with the original data space’s spatial relationships classified using the three different types of pairs described above.

An important point to note is that even though PaCMAP’s lower-dimensional embedding of the data can enable important insights into the data, the positions of the points themselves in the low-dimensional embedding are arbitrary; it is only the relationships between where the points are placed which is important. The dimensional axis in the low-dimensional embeddings does not have any units since the low-dimensional embedding combines the original dimensions in highly nonlinear and variable ways depending on the specific points and their neighbors.

B. Optimization in Spaces Defined by Neural Networks

Solving optimal control problems in neural network spaces is a challenging task. An example of the issues faced is the nonlinearities introduced by the neural network activation functions, which potentially lead to discontinuities in the representation, depending on how much care is taken to make the problem fit for optimization. The natural high-dimensional nature of the problem and the non-convex features lead us to solve our problem as a nonlinear program (NLP), choosing the solver IPOPT due to its features on large-scale problems [5]. The nonlinearities from the activation functions could cause ill-posed problems, that is, problems where the solver cannot find a proper minimum. During our investigation, we discovered that the solver could not reach solutions while using the exact Hessian. When changing to the quasi-Newton method available to us (BFGS), the solver converged to local minima. The assumption is that this is owing to the optimal control being close to being ill-posed in its current form, but further investigation into this is beyond the scope of the investigation in this paper.

Deep learning often uses the Rectified Linear Unit (ReLU) activation function, defined by $\text{ReLU}(x) = \max(0, x)$. However, ReLU is not a smooth activation function, and the derivative is zero for $x < 0$. This makes derivative-based optimization more difficult. Instead, we use the Leaky ReLU activation function,

$$\text{LeakyReLU}(x) = \begin{cases} x & \text{if } x > 0, \\ \alpha x & \text{otherwise.} \end{cases},$$

which is also not smooth, but the derivative is not zero for $x < 0$. We also use the Mish activation function [6],

$$\text{Mish}(x) = x \tanh(\ln(1 + e^x)),$$

which is both smooth and the derivative is defined $\forall x \in \mathbb{R}$.

III. METHODOLOGY

Our methodology can be summarized as follows:

- We train DRL policies using the Stable-Baselines3 [7] implementation of the Soft Actor-Critic (SAC) algorithm [8] and collect data sets using a modified version of the LunarLander-v2 environment from OpenAI Gymnasium [9]. We evaluate the policies over 1000 episodes and select policies with a high average but low minimum reward. The idea is that this will result in policies that generally perform well but fail in certain situations.

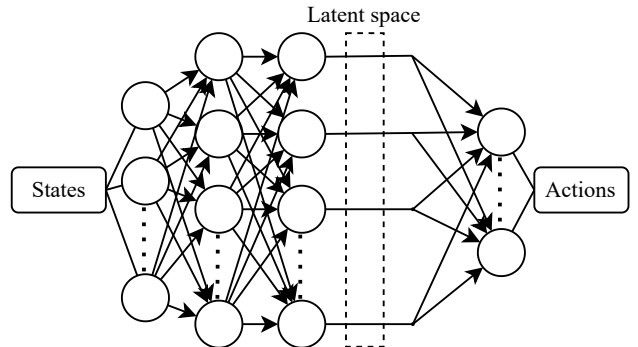


Fig. 1: Policy latent space illustration.

- From the generated data sets, we identify trajectories (episodes) where the policy crashes the vessel or fails to land in time.
- We use PaCMAP to identify successful landing episodes that are close in latent space to the unsuccessful ones.
- We then use optimization to plan a sequence of actions to move the state of the unsuccessful episode to a state close to the goal location in latent space derived from a successful episode.
- Finally, we apply the planned sequence of actions to the environment, starting from the unsuccessful episode, and observe the outcomes.

A. Problem formulation

The LunarLander-v2 environment is a reinforcement learning environment that emulates landing a spacecraft on the moon. We use the continuous version of this environment for our experiments. The agent controls the spacecraft’s main engine and side thrusters using a two-dimensional continuous action. The agent receives a reward for each step based on the lander’s position, speed, orientation, and engine usage: closer proximity to the landing pad and slower movement increase rewards while tilting away from horizontal and using engines decreases them. Landing leg contact adds points, whereas firing side or main engines deduct points per frame. The agent receives an additional reward of -100 for crashing or +100 for landing safely. An episode is considered solved if it scores a minimum of 200 points.

Using the LunarLander-v2 environment for the experiments, we want to solve the following optimization problem:

$$\begin{aligned} \min_{\mathbf{x}, \mathbf{u}} \quad & \|B_D - \pi_L(x_T)\| \\ \text{s.t.} \quad & x_{t+1} = f_e(x_t, u_t) \\ & h(x_t, u_t, t) \leq 0, \end{aligned} \quad (1)$$

where B_D is the set of latent space points in a specific latent space hypervolume, hypothesized to correspond to a desired behavioral mode, π_L is a function mapping states to latent space, i.e., all layers of the policy network except the last layer, as illustrated in Figure 1. $h(x_t, u_t, t)$ describes the path constraints, i.e., state and action limits in the reinforcement

learning (RL) environment. $f_e = \dot{x}$ is an estimation of the dynamical model of the LunarLander-v2:

$$f_e = \begin{bmatrix} x_3 \\ x_4 \\ \frac{-\sin(x_5) \cdot u_1 \cdot f_m + \cos(x_5) \cdot u_2 \cdot f_s}{m} \\ \frac{\cos(x_5) \cdot u_1 \cdot f_m + \sin(x_5) \cdot u_2 \cdot f_s - g}{m} \\ x_6 \\ c_{torque} \frac{u_2}{I} \end{bmatrix},$$

where x_1 and x_2 are the x and y positions, x_3 and x_4 are the x and y linear velocities, x_5 is the angle, and x_6 is the angular velocity. I is the inertia, m is the mass of the lander, g is the gravitational constant, and c_{torque} is a constant transforming the force to torque.

The optimal control formulation in (1) implies that we want to minimize the distance between the latent space representation of the environment state and B_D , the latent space hypervolume containing the desired behavioral mode. However, it is challenging to define B_D . Therefore, we instead optimize towards a specific point, which we hypothesize to be within B_D . We choose this latent space point using PaCMAP, and at the same time, choose x_0 , the state we initialize the optimization from.

To solve the optimization problem, we use IPOPT [5] in CasADI [10]. To use PyTorch [11] models in CasADI, we use the L4CasADi Python library [12]. The objective function is the L2 norm of the difference between the desired latent space point and the predicted latent space location at the end of the optimization horizon, as shown in (1).

B. Simplifying environments

To simplify the optimal control task, we took some steps to modify the LunarLander-v2 environment. In the original LunarLander environment, noise is added to the main thruster meant to emulate the thruster’s dispersion. We removed this noise, making the actions’ influence on the environment deterministic. We also removed the random force applied to the lander in the beginning of the episodes. Instead, we implemented a procedure for initializing the lander in a specific state for a more straightforward recreation of the particular situations we later want to investigate. We also allowed the lander to fire its side thrusters with less than 50% thrust, making the action space continuous.

IV. RESULTS AND DISCUSSION

This section shows results from using optimal control to switch the behavioral mode of a DRL agent controlling the lunar lander task described above. We use two different DRL policies, summarized in Table I. As detailed in the table, both policies are evaluated using the environment and methodology described in Section III over 1000 episodes.

	Policy A	Policy B
Activation func	torch.nn. Mish	torch.nn. LeakyReLU
Avg. reward over 1000 eval episodes	134.922	206
Hidden layer architecture	Two dense layers with 64 nodes	Two dense layers with 128 nodes

TABLE I: Data describing policies.

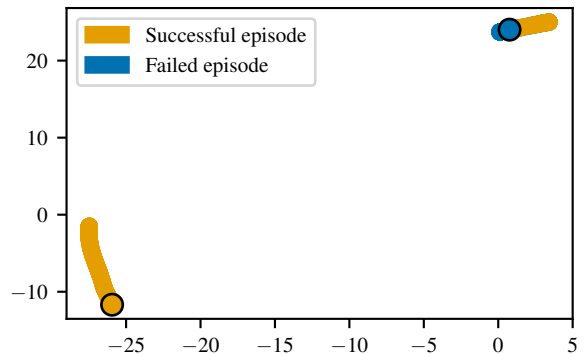


Fig. 2: Case Study 1: PaCMAP low-dimensional embedding showing latent space initial and goal location.

A. Case Study 1

During this first situation, Policy A controls the vessel. When the policy controls the vessel, the vessel falls right down and hits the ground, as seen in Figure 3b. From Figure 4, we can see that the main engine action is negative for the entirety of the situation when Policy A controls the vessel. This means that the main engine is never firing. We hypothesize that this behavior occurs because the policy never encountered a similar situation during training and, therefore, has a subpar behavior in this region of the latent space. We find another episode very close in latent space, where the policy successfully lands the agent. The main difference between these two episodes is that the vessel’s angle is closer to the neutral position during the successful episode. We visualize the latent space points for these two episodes in Figure 2 using PaCMAP. The PaCMAP algorithm clusters both the successful episode shown in orange ■ and the unsuccessful episode shown in blue ■ in the top-right corner at the start, so it is difficult to distinguish their start using this embedding. When the vessel starts to fire the main engine and correctly lands the vessel in the successful episode, the latent space representation jumps to the bottom left corner of the embedding. This indicates that the policy changes its behavioral mode here. We intervene in the failed episode at the latent space location illustrated in Figure 2 by the blue circle with a black border. This latent space location corresponds to the initial situation, as seen in Figure 3a. We want to switch the policy’s behavioral mode during the failed episode to the behavioral mode visualized in the bottom left corner in Figure 2. We use the latent space

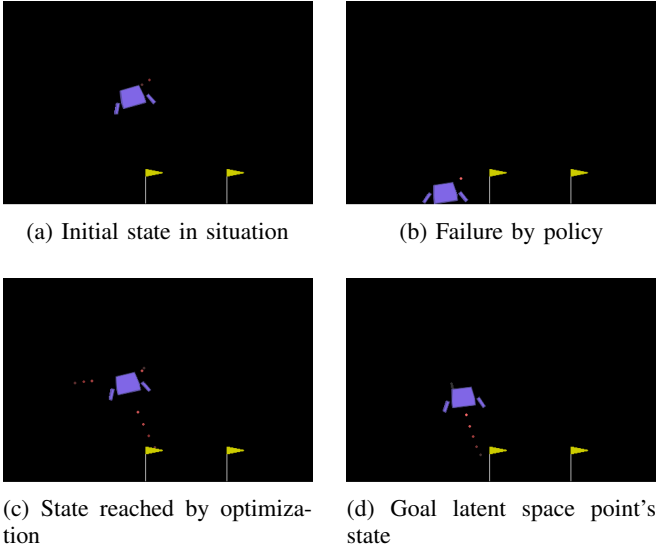


Fig. 3: Case Study 1.

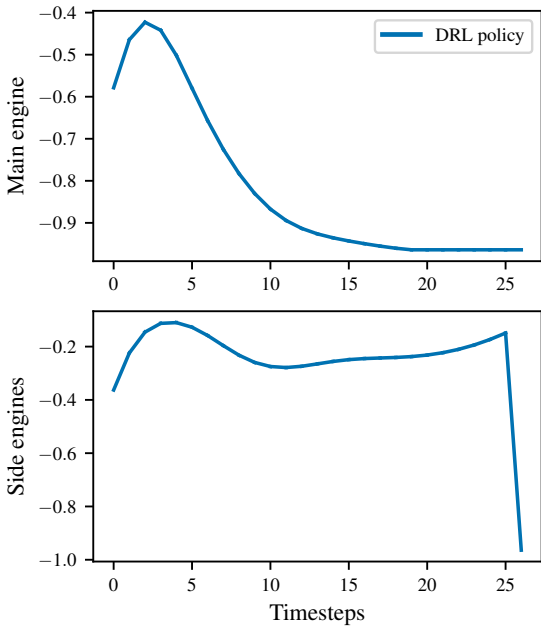


Fig. 4: Case Study 1: Actions when chosen by the policy during the failed episode.

location visualized by the orange circle with a black border, corresponding to Figure 3d, as our goal latent space location and use the optimization procedure detailed in Section III to find a sequence of actions which pushes the latent space representation of the state towards that location. The state reached can be seen in Figure 3c.

When comparing the actions chosen by the policy during the failed episode, seen in Figure 4 with the actions selected by the optimization procedure when switching the behavior, seen in Figure 3c, we can see that the way to switch the behavior involves first firing the main engine, decelerating the vessel. When comparing the side engine action, we can also

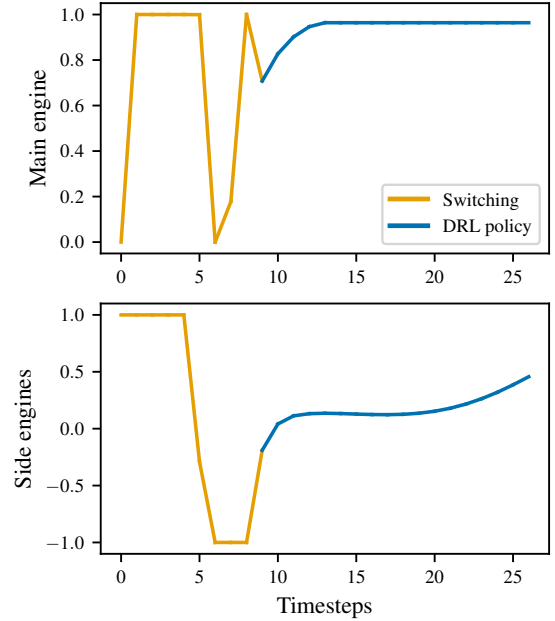


Fig. 5: Case Study 1: Actions when switching behavior.

notice that the optimization procedure fires the side engine at max. This would lead to the vessel's angle decreasing, indicating that the hypothesis regarding the vessel's angle being important for which of these behavioral modes the policy was correct.

Figure 6 shows how the optimization procedure pushes the environment towards a state much closer to the desired latent space location than ever reached during the failed episode.

The cumulative reward throughout the episode changes from -115 in the failed episode to +241 in the episode where we switch the behavioral mode using optimal control.

B. Case Study 2

In the second situation, Policy B controls the vessel. During this situation, the policy gets stuck switching cycling between four different behavioral modes, with the result being that the vessel never lands, and just hovers in place, seen in Figure 7b, and indicated by the plot of the actions in Figure 8. These four behavioral modes can be seen in the PaCMAP two-dimensional embedding of the policy's latent space in Figure 9 as the four separate blue regions of points starting in the middle of the plot and going down.

We find an episode with an initial similarity in its latent space representation, shown in orange in Figure 9. However, in this episode, the policy does not get stuck in a loop but lands the vessel successfully. Similar to in Case Study 1, we pick the initialize the optimization at the latent space location corresponding to the blue circle with black border in Figure 9, corresponding to Figure 7a, and plan a sequence of actions to move the latent space representation of the state towards the orange circle with black border, corresponding to Figure 7d.

Figure 11 shows how applying the actions from the optimization, seen in Figure 10, moves the latent space

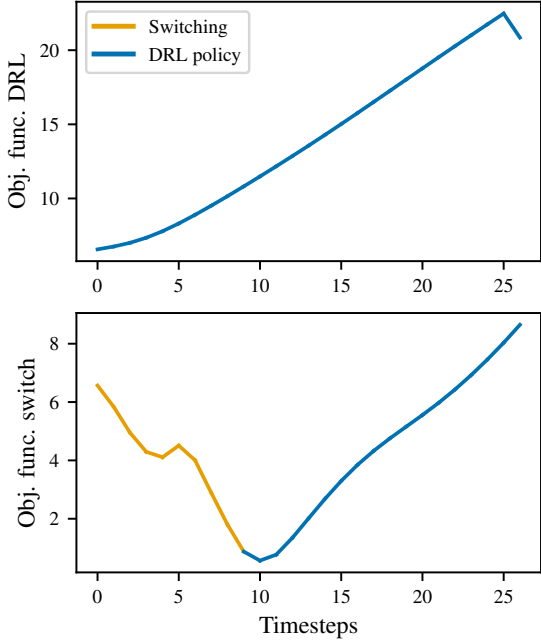


Fig. 6: Case Study 1: Objective function difference.

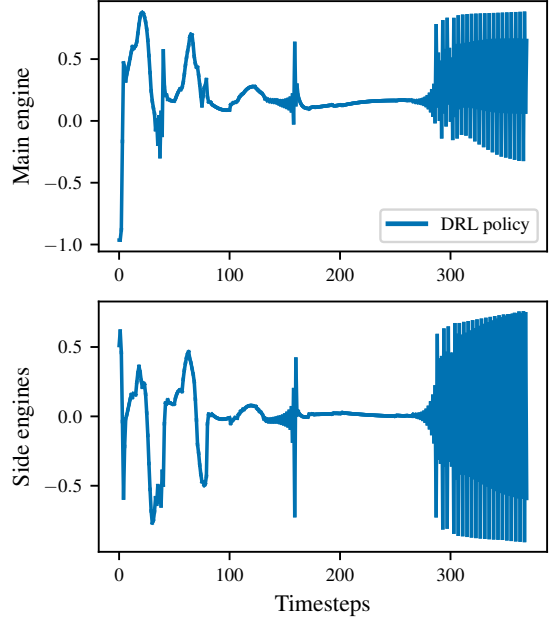


Fig. 8: Case Study 2: Actions when chosen by policy.

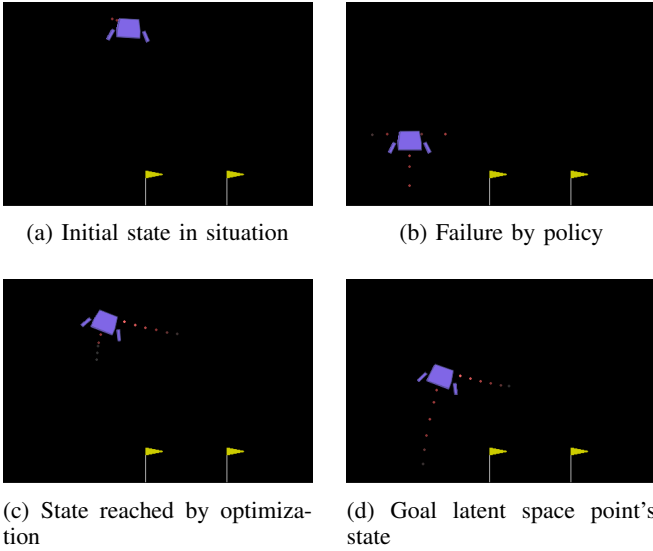


Fig. 7: Case Study 2.

representation of the environment’s state towards a location that is closer to the desired latent space location than what letting Policy B run from the initial state. The state space version of this latent space location can be seen in Figure 7c. The cumulative reward throughout the episode changes from -58 in the failed episode to +228 in the episode where we switch the behavioral mode using optimal control.

C. Moving successful behavioral mode to failed behavioral mode

To further demonstrate the ability to change the behavioral mode of the policy, we do two experiments where we do the

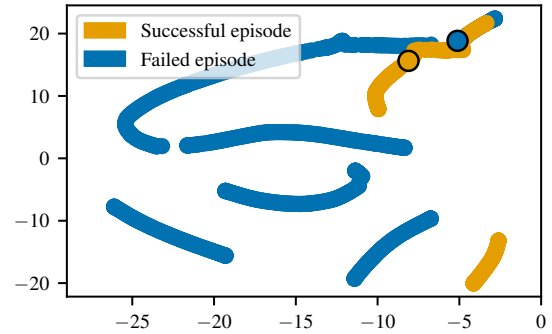


Fig. 9: Case Study 2: PaCMAP low-dimensional embedding showing latent space initial and goal location.

opposite of what we did in Case Study 1 and Case Study 2. That is, we move the policy from a successful behavioral mode to an unsuccessful behavioral mode.

For Case Study 1, we initialize in the successful episode, where the vessel has a small enough angle that the policy eventually moves to the behavioral mode in the bottom left of Figure 2. We intervene and use the optimization procedure to push the latent space representation of the state towards the failed episode, with the result being that the vessel crashes, decreasing the cumulative reward throughout the episode from +245 to -116.

For Case Study 2, we initialize the agent in the behavioral mode, which does not eventually reach where the policy gets stuck, switching between four different behavioral modes. However, we intervene and use the optimization procedure to push the latent space representation towards that region of the latent space, with the result being that the policy gets stuck similarly to in the failed episode, decreasing the cumulative

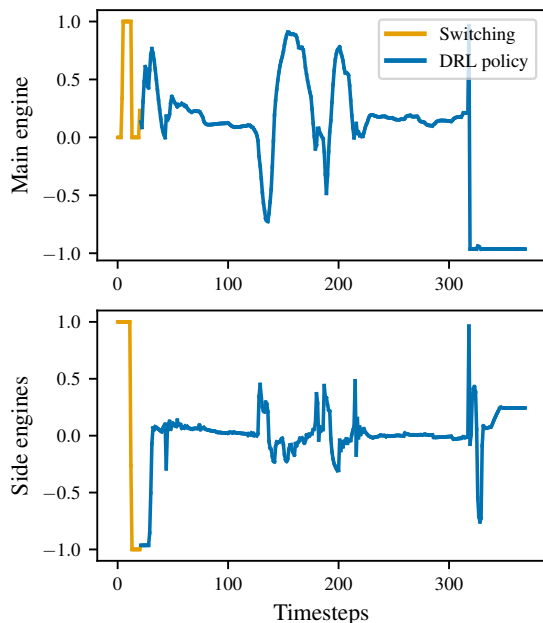


Fig. 10: Case Study 2: Actions when switching behavior.

reward throughout the episode from +233 to -79.

V. CONCLUSION

This paper has introduced a practical method for manipulating the behavioral modes of DRL policies using optimal control in the policies' latent space. Our approach demonstrates a direct way to influence the behavior of DRL policies, showing how we can switch a policy's behavioral mode to affect policy performance in simulated environments, as demonstrated with our lunar lander case study.

This work uses an analytical model of the DRL environment. However, an analytical model is not readily available for many more complex DRL environments. Further work could, therefore, involve approximating a model of the environment and then using this approximated model for optimization.

ACKNOWLEDGMENT

The Research Council of Norway supported this work through the EXAIGON project, project number 304843.

REFERENCES

- [1] A. P. Badia, B. Piot, S. Kapturowski, P. Sprechmann, A. Vitvitskiy, Z. D. Guo, and C. Blundell, "Agent57: Outperforming the atari human benchmark," in *International conference on machine learning*. PMLR, 2020, pp. 507–517.
- [2] B. R. Kiran, I. Sobh, V. Talpaert, P. Mannion, A. A. Al Sallab, S. Yogamani, and P. Pérez, "Deep reinforcement learning for autonomous driving: A survey," *IEEE Transactions on Intelligent Transportation Systems*, vol. 23, no. 6, pp. 4909–4926, 2021.
- [3] T. Salzmann, E. Kaufmann, J. Arrizabalaga, M. Pavone, D. Scaramuzza, and M. Ryll, "Real-time neural mpc: Deep learning model predictive control for quadrotors and agile robotic platforms," *IEEE Robotics and Automation Letters*, vol. 8, no. 4, pp. 2397–2404, 2023.
- [4] Y. Wang, H. Huang, C. Rudin, and Y. Shaposhnik, "Understanding How Dimension Reduction Tools Work: An Empirical Approach to Deciphering t-SNE, UMAP, TriMap, and PaCMAP for Data Visualization," *J. Mach. Learn. Res.*, vol. 22, no. 201, pp. 1–73, 2021.

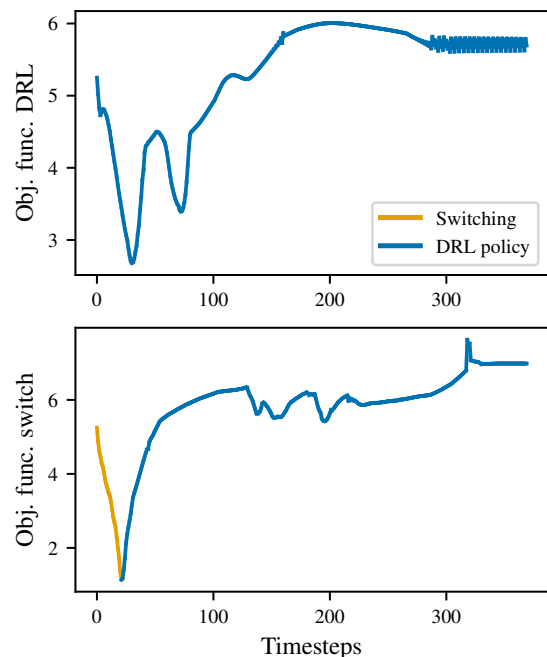


Fig. 11: Case Study 2: Objective function difference.

- [5] A. Wächter and L. T. Biegler, "On the implementation of an interior-point filter line-search algorithm for large-scale nonlinear programming," *Mathematical programming*, vol. 106, pp. 25–57, 2006.
- [6] D. Misra, "Mish: A self regularized non-monotonic activation function," *arXiv preprint arXiv:1908.08681*, 2019.
- [7] A. Raffin, A. Hill, A. Gleave, A. Kanervisto, M. Ernestus, and N. Dormann, "Stable-baselines3: Reliable reinforcement learning implementations," *J. Mach. Learn. Res.*, vol. 22, no. 268, pp. 1–8, 2021.
- [8] T. Haarnoja, A. Zhou, K. Hartikainen, G. Tucker, S. Ha, J. Tan, V. Kumar, H. Zhu, A. Gupta, P. Abbeel *et al.*, "Soft actor-critic algorithms and applications," *arXiv preprint arXiv:1812.05905*, 2018.
- [9] M. Towers, J. K. Terry, A. Kwiatkowski, J. U. Balis, G. d. Cola, T. Deleu, M. Goulão, A. Kallinteris, A. KG, M. Krimmel, R. Perez-Vicente, A. Pierré, S. Schulhoff, J. J. Tai, A. T. J. Shen, and O. G. Younis, "Gymnasium," Mar. 2023. [Online]. Available: <https://zenodo.org/record/8127025>
- [10] J. A. E. Andersson, J. Gillis, G. Horn, J. B. Rawlings, and M. Diehl, "CasADi – A software framework for nonlinear optimization and optimal control," *Mathematical Programming Computation*, 2018.
- [11] A. Paszke, S. Gross, F. Massa, A. Lerer, J. Bradbury, G. Chanan, T. Killeen, Z. Lin, N. Gimelshein, L. Antiga *et al.*, "Pytorch: An imperative style, high-performance deep learning library," *Advances in neural information processing systems*, vol. 32, 2019.
- [12] T. Salzmann, J. Arrizabalaga, J. Andersson, M. Pavone, and M. Ryll, "Learning for CasADi: Data-driven Models in Numerical Optimization," 2023.